UNIVERSITY
OF
QUEENSLAND

Department of Civil Engineering

RESEARCH REPORT SERIES

The Behaviour of Cylindrical Guyed Stacks Subjected to Pseudo-Static Wind Loads

P. SWANNELL

Research Report No. CE41
March, 1983

CIVIL ENGINEERING RESEARCH REPORTS

This report is one of a continuing series of Research Reports published by the Department of Civil Engineering at the University of Queensland. This Department also publishes a continuing series of Bulletins. Lists of recently published titles in both of these series are provided inside the back cover of this report. Requests for copies of any of these documents should be addressed to the Departmental Secretary.

The interpretations and opinions expressed herein are solely those of the author(s). Considerable care has been taken to ensure the accuracy of the material presented. Nevertheless, responsibility for the use of this material rests with the user.

Department of Civil Engineering,
University of Queensland,
St Lucia, Q 4067, Australia,
[Tel:(07) 377-3342, Telex:UNIVQLD AA40315]

THE BEHAVIOUR OF CYLINDRICAL GUYED STACKS SUBJECTED TO PSEUDO-STATIC WIND LOADS

by

P. SWANNELL, BSc*(Brist.)*, PhD*(Birm.)*, MICE, FAWI, MIEAust,

Reader in Civil Engineering

RESEARCH REPORT NO. CE 41

Department of Civil Engineering

University of Queensland

March 1983

Synopsis

The Report describes a non-linear elastic analysis procedure for guyed masts or stacks of cylindrical cross-section. The analysis is an extension of original work by Poskitt and Livesley (1963) and accounts for behaviour due to lateral wind on the guy ropes and stack. Stack wind loads are described by a power law which represents current procedures described in SAA Loading Code Part 2 - Wind Forces, AS1170. Destabilising effects of the axial thrust in the stack are properly accounted for, and the guy ropes are represented as shallow parabolas with guy tensions therefore described by the customary cubic equation. Additional stack loading due to temperature effects and gravity are also included.

An investigation of the influence of wind direction upon system performance is described and conclusions are drawn regarding the choice of critical wind directions for design purposes.

CONTENTS

1. INTRODUCTION

A full investigation of the response of a slender guyed flare stack or mast calls for both dynamic and static analyses. Proposed design dimensions, stack diameter, taper geometries, guy sizes, erection tensions and anchorage positions are first investigated by static analysis, with loads arising from self-weight, ice accretion, temperature changes, etc. These static loads are supplemented by wind loads on the stack and the guys and the wind loads are only "pseudo-static". It may be necessary, subsequently, to perform dynamic analyses in order to ascertain natural frequencies and responses to wind-induced oscillations.

This paper is concerned with the static analysis. Approximate methods of analysis incorporating fairly crude assumptions regarding guy rope stiffness and utilising very idealised wind distributions have been in existence for many years, e.g. Bamber (1956). With the advent of readily available computing power more sophisticated analysis became a realistic proposition. Poskitt and Livesley (1963) presented a fundamentally sound non-linear elastic analysis incorporating the effects of idealised wind-loading on both stack and guy elements, in the context of cylindrical stacks.

In an unpublished Report (1969) Swannell and Spooner extended this work to include a stack wind distribution obeying a power law similar to that incorporated in current British and Australian wind codes. Non-linear elastic effects due to the destabilising action of axial loads and non-linear guy rope response are retained in this analysis which also incorporates automatic idealisation facilities to permit taper elements and minimise user input requirements. This analysis has recently been updated by the Author to include operation in metric units and totally incorporate the current AS1170 Part 2 wind loading provisions. The basis

of the analysis is described below and results have been obtained using the program METGUM (1982).

A typical cylindrical stack has been chosen and its response to Terrain Category 3 wind conditions has been investigated. The basic design wind speed is 50 m/s corresponding to a 50 year return period in the Brisbane area. The influences of wind direction and guy erection tensions are the principle subjects of investigation and a complete description of the trial structure and the design parameters is given in Figures 1 and 2 and Table 1.

The investigation is, in some measure, specific to the chosen stack geometry and the particular guy rope stiffnesses and is influenced in part by the chosen gravity and temperature loadings. This is unavoidable. The complexity of the response and the multiplicity of design variables is such that it is not possible to present results in generalised or non-specific terms. However the particular structure has been realistically chosen (being based on a particular as-built stack) with sufficient simplification regarding guy rope symmetry and the absence of tapers to leave the fundamental behaviour unobscured by secondary effects.

2. ANALYTICAL PROCEDURE

The analysis is a non-linear elastic, small displacement, analysis in which the stack is idealised as an assembly of prismatic beam-column elements inter-connected at nodes corresponding to each guying point or change of stack cross-sectional geometry. Element stiffness is described by the "exact s and c function" first order non-linear elastic element stiffness matrices based on the original work by Livesley and Chandler (1956). The results are summarised in Appendix C.

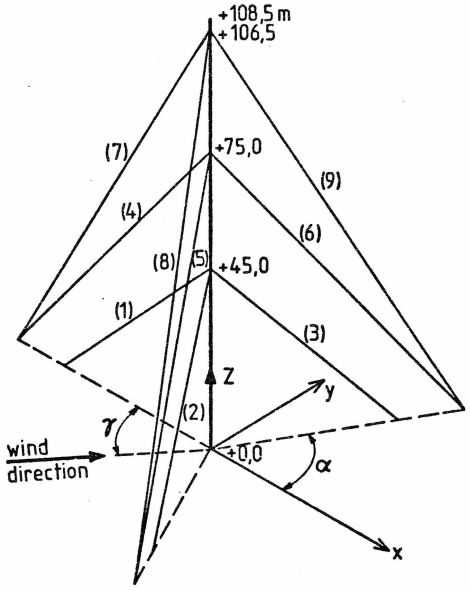

FIGURE 1 : Stack and guy geometry

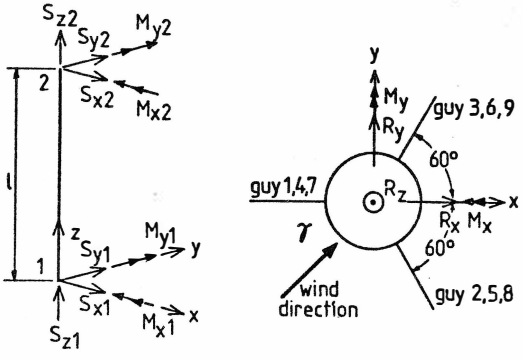

(a) Element End Forces (b) Nodal Loads

FIGURE 2 : Nodal forces and guy arrangement

TABLE 1 : Table design values

Guy No.	Radius to Anchorage (m)	Height to Guy Point (m)	Angle α^o
1	45.5	45.5	180^o
2	45.5	45.0	300^o
3	45.5	45.0	60^o
4	60.5	75.0	180^o
5	60.5	75.0	300^o
6	60.5	75.0	60^o
7	60.5	106.5	180^o
8	60.5	106.5	300^o
9	60.5	106.5	60^o

Diam. of all ropes	= 25 mm
Weight per metre run	= 0.035 kN
Effective Y.M.	= 100 kN/mm^2
Drag coefficient	= 1.2

(a) Guy Rope Data

Outside Diameter (constant)	= 1200 mm
Wall Thickness (constant)	= 25 mm
Young's Modulus	= 200 GPa
Eff. Diam. (for wind)	= 1200 mm
Diameter above 106.5 m	= 1400 mm
Weight above 106.5 m	= 11.1 kN
Ambient Temperature	= 20^{o}C
Temperature at Stack Bottom	= 150^{o}C
Temperature at Stack Top	= 38^{o}C
Specific Weight of Stack	= 77 kN/m^3
Ice Accretion	= zero
Base Support Conditions	= fully fixed

Wind Loading Conditions:
T.C. 3, 50 year return period, Brisbane
Wind Incidence Angles = $0 \rightarrow 60^o$ in 5^o increments

Erection Tensions:
Erection tensions vary from 20 kN to 50 kN (identical in each rope) in 5 kN increments.

(b) Stack Data and Load Cases

Non-linearity also arises from the guy rope behaviour. The ropes are assumed to hang as catenaries sufficiently flat to be represented by a portion of a parabola for calculation purposes. The resulting guy rope tensions are described by cubic equations and are functions of the lateral loads on the guys, the initial erection tensions and the guying point displacements. A modified Newton-Raphson approach is used in the solution of the linearised governing equations with iteration until all response output is sufficiently converged.

The governing equations are the conventional ones, viz.

$$\{R\} = [K]\{r\} \tag{1}$$

in which, in the present analysis, [K] is the conventional assembly of stack element stiffness matrices, {r} is the output displacement response and {R} is the sum of two contributions, viz.

$$\{R\} = \{R_1\} + \{R_2\} \tag{2}$$

where $\{R_1\}$ = Vector of kinematically equivalent nodal loads, due to stack wind, temperature effects and gravity

and $\{R_2\}$ = Vector containing loads ex. guy ropes and terms which account for the spring constraints offered by the guys.

The development of $\{R_1\}$ and $\{R_2\}$ is the essence of the analysis and is described below.

3 THE LOAD VECTOR {R}

Contributions to $\{R_1\}$ arise from gravity loads, temperature effects and lateral wind on the stack. Gravity loads and temperature effects are treated in an entirely standard way but the wind loading requires further description.

3.1 Wind Loads on the Stack

Noting the requirements of AS1170, Part 2 (pages 7-10) it follows that the appropriate wind distribution up the stack is a "power law" of the form

$$w = k_w.Z^n \qquad (kN/m) \qquad (3)$$

For Terrain Category 3 loading, in which the gradient height Z_g = 400 metres and a basic design wind speed = 50 m/s, it may be deduced that n = 0.28 and $k_w = 0.5107\ C_p.d_e$ where C_p = 0.8 for a long relatively smooth stack and d_e = effective diameter of the stack.

The analysis uses this power law and consequently the contributions to $\{R_1\}$ must be consistently computed by determination of the precise "fixed end" behaviour of a typical stack element carrying this general lateral load in the presence of a destabilising axial load. This is a challenging little piece of analysis described fully elsewhere (Swannell and Spooner 1969) and the results for a typical element are given in Appendix C. It should be noted that the results call for numerical integration and this is achieved automatically in the program using Simpson's Rule.

The vector $\{R_1\}$ is assembled by routine procedures on the basis of these results and in the presence of destabilising axial loads which are *initially* assumed to arise from gravity, temperature effects and guy rope tensions with *zero* displacements of all nodes. Subsequent modification of the axial loads occurs as successively better approximations to the equilibrium set of loads become available during iteration.

3.2 The computation of $\{R_2\}$

Vector $\{R_2\}$ contains nodal loads ex. guy ropes modified by terms which account for the guy rope stiffnesses.

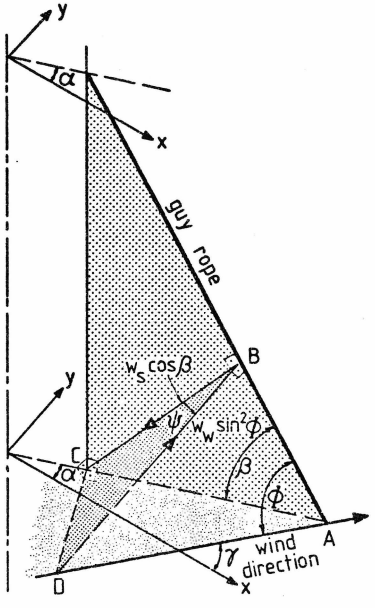

FIGURE 3 : Normal loads on a guy rope

Figure 3 shows a typical guy rope in which loads normal to the rope arise from self-weight (W_s) and wind (W_w). The resultant normal load acting on the guy is W_n. W_w is the usual drag force per unit length and its component normal to the guy rope is assumed to be $W_w \sin^2 \phi$ where ϕ is the true angle between a guy rope and the incident wind. The result for W_n is given in Appendix C.

Guying rope behaviour is developed on the basis that the stack is erected in still air with erection tensions being T_E. If, due to imposition of the design loads, the span of a guy (measured in the direction of the guy) increases by an amount δ then the induced guy tension, T, is given by a cubic equation, viz.

$$T^3 + E_G A_G T^2 \left\{ \frac{W_{NE}^2}{24 T_E^2} - \frac{T_E}{E_G A_G} - \frac{\delta}{L} \right\} - \frac{E_G A_G}{24} W_N^2 = 0 \qquad (4)$$

where W_{NE} = "still air" lateral load (gravity only)

W_N = design lateral load due to wind and gravity

$E_G A_G$ = guy rope axial stiffness.

Equation (4) with $\delta = 0$ gives guy rope tensions, T_o, in the absence of nodal displacements. Equation (4) may then be re-phrased in terms of T_o, viz.

$$T^3 + T^2 \left\{ \frac{\bar{K}}{T_o^2} - T_o - \frac{E_G A_G}{L} \delta \right\} - \bar{K} = 0 \qquad (5)$$

where $\bar{K} = \frac{E_G A_G W_N^2}{24}$

Equation (5) may be linearised for use in the n th iteration cycle as

$$T_n = \tau_{n-1} + \mu_{n-1} (\delta_n - \delta_{n-1}) \tag{6}$$

where τ_{n-1} = tension given by Equation (5) with $\delta = \delta_{n-1}$, the estimate of δ at the completion of the (n-1) th iteration cycle. μ_{n-1} is the value of $dT/d\delta$ when $\delta = \delta_{n-1}$ viz.

$$\mu_{n-1} = \frac{E_G A_G}{L} \left\langle \frac{\tau^3_{n-1}}{\tau^3_{n-1} + 2\bar{K}} \right\rangle \tag{7}$$

Hence,

$$T_n = T'_{n-1} + \mu_{n-1}\, \delta_n \tag{8}$$

in which $T'_{n-1} = \tau_{n-1} - \mu_{n-1}\, \delta_{n-1}$ and both T'_{n-1} and μ_{n-1} are known at the commencement of the n th iteration cycle.

Denoting the guy rope tensions at the i th guying point, in the n th iteration cycle, as $\{T_{n,3i-2}\ T_{n,3i-1}\ T_{n,3i}\}$ the consequential stack forces at this guying point become,

$$\{R_{Gi}\} = [T]\{T_{n,3i-2}\ T_{n,3i-1}\ T_{n,3i}\} \tag{9}$$

where $\{R_{Gi}\} = \{R_x R_y R_z M_x M_y\}$ at the i th point.

The transformation matrix [T] is given in Appendix C. It follows that the guy rope extensions are related to the stack displacements at the i th guy point by,

$$\{\delta\} = -[T]^t \{r_i\} \tag{10}$$

where $\{\delta\} = \{\delta_{n,3i-2}\ \delta_{n,3i-1}\ \delta_{n,3i}\}$

and $\{r_i\} = \{u_i v_i w_i \theta_{xi} \theta_{yi}\}$

Using Equations (8) and (9),

$$\{R_{Gi}\} = [T]\{T'_{n-1}\} - [T]\lceil\mu_{n-1}\rfloor[T]^t\{r_i\} \qquad (11)$$

where $\{T'_{n-1}\}$ implies a 3 x 1 vector of modified guy tensions at point i and $\lceil\mu_{n-1}\rfloor$ is a 3 x 3 diagonal array of guy stiffnesses.

The vector $\{R_2\}$ contains all $\{R_{Gi}\}$ together with zero elements at row positions not associated with a guy point.

4. FINAL STACK MOMENTS AND DISPLACEMENTS

The iterative solution of Equation (1), with the second term of Equation (11) incorporated into a modified structure stiffness matrix, gives all the nodal displacements. Element end forces and displacements are then obtained by substitution into element stiffness relationships. It remains, then, to obtain bending moment distributions throughout the stack, noting that this requires the contribution from the axial load and, therefore, a full solution of the equation of the deflected shape of each element.

This solution, in the presence of axial load and a "power law" lateral load has been obtained by the author and the results in terms of element end displacements are given in Appendix C. Final program output includes moments, axial loads and displacement components throughout the stack together with final guy rope tensions.

5. ANALYTICAL RESULTS

The objective has been to produce data regarding the influence of wind direction and erection tensions. Results have been obtained for wind directions defined by $\gamma = 0^{o}$ through $\gamma = 60^{o}$ in 5^{o} increments (see Figures 1 and 2). All values of $\gamma > 60^{o}$ simply repeat these solutions. Erection tensions have been varied in the range 20 kN through 50 kN with all guys possessing the same erection tension for any one analysis.

Figure 4 shows the effect of wind angle upon base moments, using various erection tensions. It is always the base moment which is the largest moment acting on the stack. The critical wind angle for the production of maximum moment is $\gamma = 0^{o}$ for erection tensions greater than about 26 kN. For lower tensions the critical angle gets progressively bigger as the tension reduces, with $\gamma \doteqdot 40^{o}$ at the lowest trial tension.

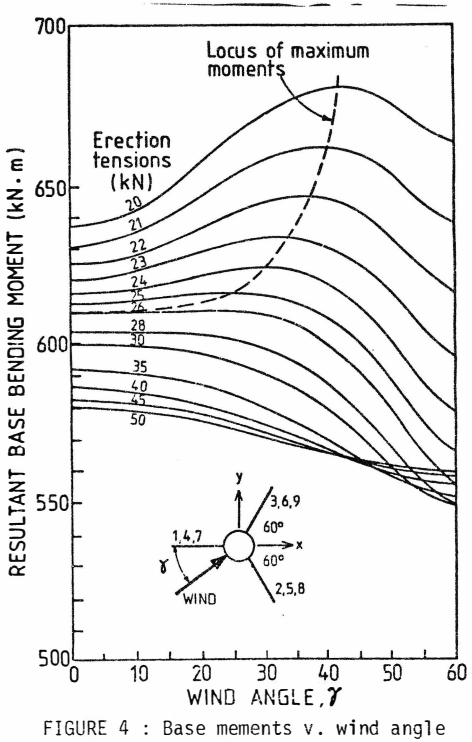

FIGURE 4 : Base mements v. wind angle

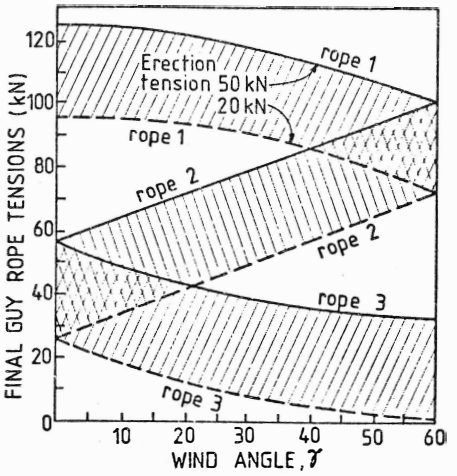

FIGURE 5 : Final guy rope tensions v. wind angle (guys 1, 2, 3)

Note from Figures 5, 6 and 7 that the chosen range of erection tensions is entirely realistic and 20 kN represents a lowest acceptable value (under the particular design conditions) for which a slack guy condition is avoided. Figures 5 and 6 highlight the influence of wind angle upon final guy tensions.

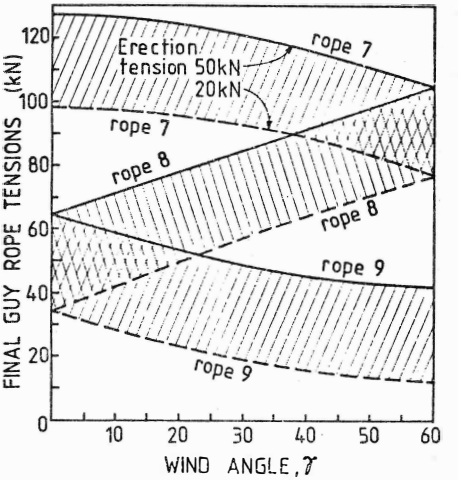

FIGURE 6 : Final guy rope tensions v. wind angle (guys 7, 8, 9)

Figures 5 and 6 define the range of guy tensions experienced by the three lowest and the three highest ropes respectively. It can be noted that the range of final tensions in any guy, for any particular wind angle, mirrors approximately the range of erection tensions. For high erection tensions, the final tensions experienced by the guys lie in the range approximately 2.5 x erection tension down to 0.5 x erection tension as the wind angle varies. For low erection tensions the corresponding range is from about 5 x erection tension down to near-slack condition.

Figure 7 is an alternative presentation in which the near-linear relationship between erection tension and final tension is highlighted.

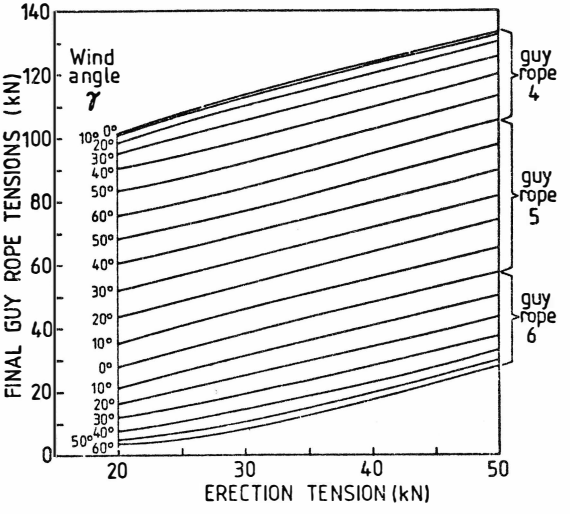

FIGURE 7 : Final guy rope tension v. erection tension (guys 4, 5, 6)

Figures 8 to 11 give more details of stack behaviour.

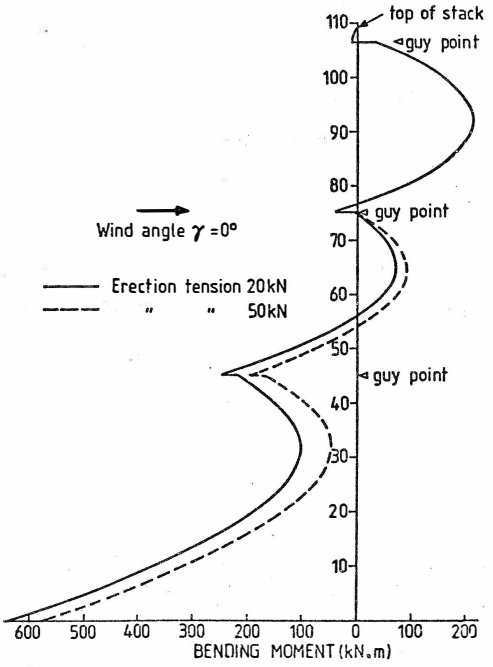

FIGURE 8 : Typical bending moment diagram with γ = 0

Figure 8 shows a typical bending moment diagram for $\gamma = 0^{o}$ i.e. with bending in a vertical plane containing the wind and guys 1, 4 and 7. Note that for low erection tensions, this diagram does *not* incorporate the biggest resultant moment at any stack position since Figure 1 highlights the fact that maximum moments then occur with values of $\gamma > 0^{o}$. For example, with $\gamma = 40^{o}$ and T_E = 20 kN maximum stack resultant moments can exceed those shown in Figure 8 by up to 7%.

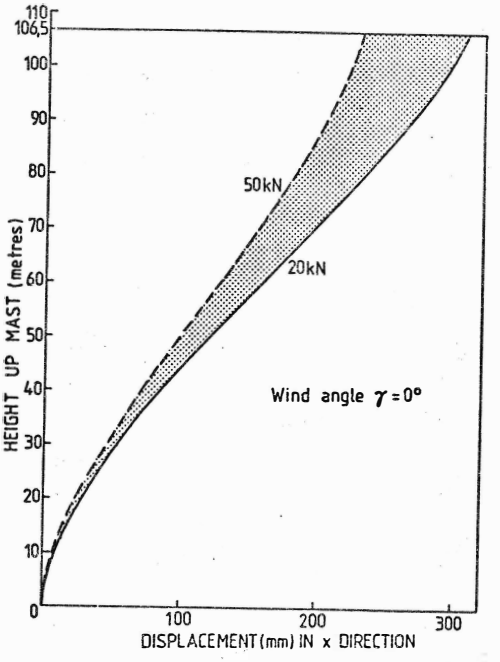

FIGURE 9 : Displaced shape of stack

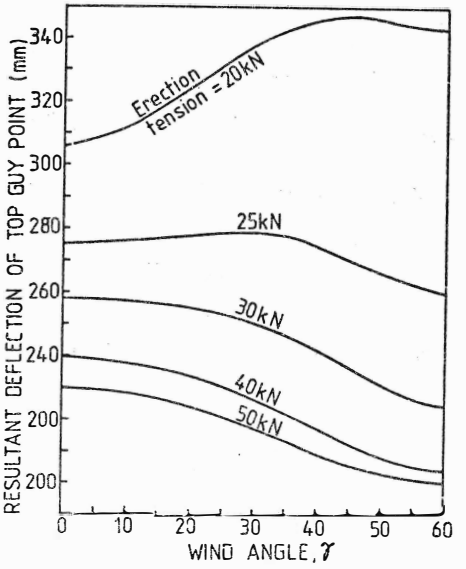

FIGURE 10 : Resultant top guy point deflexion

Figure 9 shows stack displacements for $\gamma = 0^{o}$. It should be read in conjunction with Figure 10 where the influence of wind angle upon stack tip deflexion is displayed. Again, Figure 10 shows that tip deflexions at $\gamma = 0$ are exceeded when $\gamma > 0$ for low erection tensions.

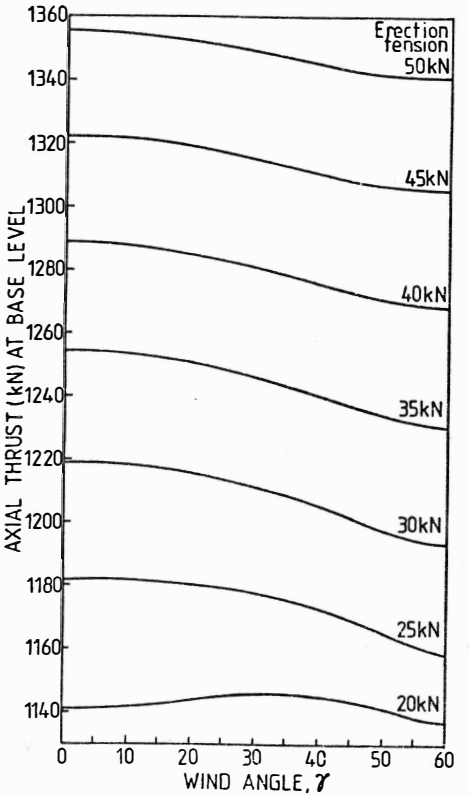

FIGURE 11 : Axial thrusts v. wind angle

Finally, Figure 11 plots the base thrusts as a function of wind angle and it may be seen that thrusts associated with $\gamma = 0$ are generally, but not always the largest. The thrust values are generally insensitive to wind angle and only vary by about 2% throughout the range $\gamma = 0$ through 60^{o}.

6. CONCLUSION

The results demonstrate the type of static response that might be anticipated in a guyed stack or mast and provide insight into the proper choice of wind direction and erection tension. Tapers have not been included in the analyses and the provision of a short stockier base section to the stack may contribute some stiffening effect but will also "attract moment". Effects are likely to be small compared with those obtained by talented juggling of the guy parameters.

Obviously the apparent axial stiffness of the taut guy rope ($E_G A_G$) is crucial and must be carefully estimated before an analysis is undertaken. The present analysis includes a value of E_G which is approximately 50% of a "solid steel" value.

It must be noted that the erection tensions chosen for this analysis are influenced by the contribution of suppressed temperature expansion in the hot stack. The effect of the elevated stack temperature is effectively to increase the erection tensions, thus stiffening the support system. A countering effect is the consequential increase in compressive, destabilising stack axial loads. There is no doubt that reanalysis without temperature effects included will make significant quantitative changes in the results with the stack possessing significantly *greater* base moments and larger tip deflexions. However, the qualitative influence of the design variables γ and T_E remains the same. With the program METGUM it is possible to obtain a wide selection of output responses with and without temperature effects and, for example, using non-symmetrical guy rope configurations. For the cost of a few cents per analysis (or at no cost on a stand-alone micro-computer possessing a good FORTRAN system) the designer may investigate a very wide range of alternatives.

APPENDIX A - REFERENCES

1. BAMBER, D. (1956) The Design of Towers, Masts and Pylons. The Association of Engineering and Shipbuilding Draughtsmen, Richmond, Surrey, U.K.

2. LIVESLEY, R.K. and CHANDLER, D.B. (1963) Stability Functions for Structural Frameworks. Manchester University Press.

3. POSKITT, T.J. and LIVESLEY, R.K. (1963) "Structural analysis of guyed masts". Proc. Inst. Civ. Eng., Vol. 24, pp 373-386.

4. STANDARDS ASSOCIATION OF AUSTRALIA (1973). SAA Loading Code Part 2 - Wind Forces. AS1170.

5. SWANNELL, P. and SPOONER, J.B. (1969) "A general analysis package for the elastic behaviour of statically loaded guyed masts and stacks. Univ. of Birmingham, Dept of Civil Engineering. 33 p.

6. SWANNELL, P. (1982) METGUM, a FORTRAN program for the analysis of cylindrical masts and stacks subjected to AS1170 wind loading. Univ. of Qld., Dept of Civil Engg.

APPENDIX B - NOMENCLATURE

The following is a list of main symbols used in the body of the text.

Symbols used in Appendix C are generaly defined therein.

Symbol	Meaning
A	cross-sectional area of stack element
A_G	Cross-sectional area of guy rope
C_D	drag coefficient
E	Young's modulus of stack material
E_G	apparent Young's modulus of guy rope
I_x, I_y	second moments of area, stack cross-section
$[K]$	structure stiffness matrix
$\bar{K}$	see Equation (5)
L	guy rope length
M_x, M_y, M_z	element end moments
R	nodal load vector
R_1	load contribution ex wind, gravity etc.
R_2	load contribution ex guys etc
R_{Gi}	loads ex guys at ith guy point
R_x, R_y, R_z	components of R_{Gi}
T	guy tension
T_E	guy erection tension in still air
T_o	guy tension ex erection plus lateral loads with zero nodal displacements
T_n	linearised tension (nth iteration)
T^1_{n-1}	see Equation (8)
W_N	normal load on guy rope ex wind and gravity
W_{NE}	normal load on guy rope in still air
Z	height coordinate
Z_g	gradient height (AS1170)

Symbol	Meaning
d_e	effective stack diameter for wind purposes
k_w	wind load coefficient
l	stack element length
n	wind load index, or iteration counter as appropriate
u_i, v_i, w_i	nodal displacements
w	wind load/unit length
$[T]$	transformation matrix (tensions)
γ	wind angle w.r.t. x axis
δ	guy rope extension
μ_{n-1}	$dT/d\delta$, $\delta = \delta_{n-1}$
τ_{n-1}	tension as given by Equation (5) $(n-1)$th iteration
$\theta_{x_1}, \theta_{y_1}$	nodal rotations

APPENDIX C - SOME ESSENTIAL RELATIONSHIPS

(i) Element Stiffness Matrix

With element end force vector $\{s_{x1}\ s_{y1}\ s_{z1}\ m_{x1}\ m_{y1}\ s_{x2}\ s_{y2}\ s_{z2}\ m_{x2}\ m_{y2}\}$

$$[k] = \left[\begin{array}{c|c} k_{11} & k_{12} \\ \hline k_{21} & k_{22} \end{array}\right] \quad \text{where } k_{11},\ k_{12},\ k_{21},\ k_{22} \text{ are given below:}$$

$$[k_{11}] = \begin{bmatrix} \frac{B_1 EI_Y}{\ell^3} & 0 & 0 & 0 & \frac{B_2 EI_Y}{\ell^2} \\ 0 & \frac{B_1 EI_X}{\ell^3} & 0 & \frac{B_2 EI_X}{\ell^2} & 0 \\ 0 & 0 & \frac{EA}{\ell} & 0 & 0 \\ 0 & \frac{B_2 EI_X}{\ell^2} & 0 & \frac{B_3 EI_X}{\ell} & 0 \\ \frac{B_2 EI_Y}{\ell^2} & 0 & 0 & 0 & \frac{B_3 EI_Y}{\ell} \end{bmatrix}$$

$$[k_{22}] = \begin{bmatrix} \frac{B_1 EI_Y}{\ell^3} & 0 & 0 & 0 & \frac{-B_2 EI_Y}{\ell^2} \\ 0 & \frac{B_1 EI_X}{\ell^3} & 0 & \frac{-B_2 EI_X}{\ell^2} & 0 \\ 0 & 0 & \frac{EA}{\ell} & 0 & 0 \\ 0 & \frac{-B_2 EI_X}{\ell^2} & 0 & \frac{B_3 EI_X}{\ell} & 0 \\ \frac{-B_2 EI_Y}{\ell^3} & 0 & 0 & 0 & \frac{B_3 EI_Y}{\ell} \end{bmatrix}$$

$$[k_{12}] = [k_{21}]^t = \begin{bmatrix} -\frac{B_1 EI_Y}{\ell^3} & 0 & 0 & 0 & \frac{B_2 EI_Y}{\ell^2} \\ 0 & -\frac{B_1 EI_X}{\ell^3} & 0 & \frac{B_2 EI_X}{\ell^2} & 0 \\ 0 & 0 & -\frac{EA}{\ell} & 0 & 0 \\ 0 & -\frac{B_2 EI_X}{\ell^2} & 0 & \frac{B_4 EI_X}{\ell} & 0 \\ -\frac{B_2 EI_Y}{\ell^2} & 0 & 0 & 0 & \frac{B_4 EI_Y}{\ell} \end{bmatrix}$$

The stability functions B_1, B_2, B_3 and B_4 are defined below:

$$B_1 = \frac{2s(1 + c)}{m} = 2s(1 + c) - 4\alpha_o^2$$

$$B_2 = s(1 + c)$$

$$B_3 = s$$

$$B_4 = sc$$

where

$$\alpha_o = \frac{\pi}{2}\sqrt{\rho}, \qquad \rho = \frac{\text{Axial Thrust}}{\text{Euler Load}}$$

$$s = \frac{(1 - 2\alpha_o \cot 2\alpha_o)\alpha_o}{\tan \alpha_o - \alpha_o}$$

$$m = \frac{2s(1 + c)}{2s(1 + c) - 4\alpha_o^2}$$

$$c = \frac{2\alpha_o - \sin 2\alpha_o}{\sin 2\alpha_o - 2\alpha_o \cos 2\alpha_o}$$

(ii) Element Fixed End Forces

The expressions for fixed-end moments and shears acting on a stack element (see Fig. 2) due to wind are:

$$m_{1X}^F = \frac{-k_w \sin\gamma}{(n+1)(n+2)} \{H_1^{n+2} + \bar{m}_X^2 B_X\}$$

$$m_{1Y}^F = \frac{-k_w \cos\gamma}{(n+1)(n+2)} \{H_1^{n+2} + \bar{m}_Y^2 B_Y\}$$

$$m_{2X}^F = \frac{k_w \sin\gamma}{(n+1)(n+2)} \{H_2^{n+2} + \bar{m}_X^2 B_X - \bar{m}_X^3 C_X \ell\}$$

$$m_{2Y}^F = \frac{k_w \cos\gamma}{(n+1)(n+2)} \{H_2^{n+2} + \bar{m}_Y^2 B_Y - \bar{m}_Y^3 C_Y \ell\}$$

$$S_{1X}^F = \frac{k_w \cos\gamma}{(n+1)} \{H_1^{n+1} - \frac{C_Y \bar{m}_Y^3}{(n+2)}\}$$

$$S_{1Y}^F = \frac{k_w \sin\gamma}{(n+1)} \{H_1^{n+1} - \frac{C_X \bar{m}_X^3}{(n+2)}\}$$

$$S_{2X}^F = \frac{-k_w \cos\gamma}{(n+1)} \{H_2^{n+1} - \frac{C_Y \bar{m}_Y^3}{(n+2)}\}$$

$$S_{2Y}^F = \frac{-k_w \sin\gamma}{(n+1)} \{H_2^{n+1} - \frac{C_X \bar{m}_X^3}{(n+2)}\}$$

Definition of symbols:

γ = Angle of incidence of wind, measured as shown in Fig. 2

H_1 = Height of end 1 from base

H_2 = Height of end 2 from base

$\bar{m}_X, \bar{m}_Y = \sqrt{\frac{\text{Axial load in element}}{E \times I}}$, $\bar{m}_X$ use I_X; $\bar{m}_Y$ use I_Y } equal in circular section

$$B_X, B_Y = \frac{-I'(\sin\bar{m}\ell - \bar{m}\ell\cos\bar{m}\ell) - J'(1 - \cos\bar{m}\ell - \bar{m}\ell\sin\bar{m}\ell)}{2(1-\cos\bar{m}\ell) - \bar{m}\ell\sin\bar{m}\ell}$$

$$C_X, C_Y = \frac{-I'(1-\cos\bar{m}\ell) + J'\sin\bar{m}\ell}{2(1-\cos\bar{m}\ell) - \bar{m}\ell\sin\bar{m}\ell}$$

In the above $\bar{m}$, I' and J' take the suffices 'x' and 'y' corresponding to B_X, C_X and B_Y, C_Y respectively. For circular sections $C_X = C_Y$, $B_X = B_Y$, $I'_X = I'_Y$, $J'_X = J'_Y$, although in the computer programme, for generality, they are computed separately.

I' and J' are defined as below:

$$I' = \frac{1}{\bar{m}} \int_0^{\ell} (H_1 + z)^{n+2} \cos \bar{m}z.dz$$

$$J' = \frac{1}{\bar{m}} \int_0^{\ell} (H_1 + z)^{n+2} \sin \bar{m}z.dz$$

} suffices X or Y used throughout

k_w, n are defined in Equation (3).

(iii) Resultant Lateral Load on Guy Rope (see Fig. 3)

If W_N = Total normal (wind + gravity) load on the guy then:

$$W_N = L \sqrt{M^2 + N^2}$$

where

$$M = w_W \sin\beta \cos(\gamma-\alpha) \sqrt{\sin^2\beta \cos^2(\gamma-\alpha) + \sin^2(\gamma-\alpha)} - w_S \cos\beta$$

$$N = w_W \sin(\gamma-\alpha) \sqrt{\sin^2\beta \cos^2(\gamma-\alpha) + \sin^2(\gamma-\alpha)}$$

L = length of the guy

(iv) Transformation Matrix [T]

$$[T] = \begin{bmatrix} \cos\beta_{3i-2} \cos\alpha_{3i-2} & \cos\beta_{3i-1} \cos\alpha_{3i-1} & \cos\beta_{3i} \cos\alpha_{3i} \\ \cos\beta_{3i-2} \sin\alpha_{3i-2} & \cos\beta_{3i-1} \sin\alpha_{3i-1} & \cos\beta_{3i} \sin\alpha_{3i} \\ -\sin\beta_{3i-2} & -\sin\beta_{3i-1} & -\sin\beta_{3i} \\ d\sin\beta_{3i-2} \sin\alpha_{3i-2} & d\sin\beta_{3i-1} \sin\alpha_{3i-1} & d\sin\beta_{3i} \sin\alpha_{3i} \\ d\sin\beta_{3i-2} \cos\alpha_{3i-2} & d\sin\beta_{3i-1} \cos\alpha_{3i-1} & d\sin\beta_{3i} \cos\alpha_{3i} \end{bmatrix}$$

(v) Final Stack Displacements, Moments and Shears

Bending Moments @ the x and y axes at a distance Z from the lower end of any stack element are:

(a) About the x axis:

$$BMX = M_{X_1} - S_{Y_1} \cdot Z + S_{Z_1} (v_Z - v_1) - M_{WX}$$

(b) About the y axis:

$$BMY = M_{Y_1} - S_{X_1} \cdot Z + S_{Z_1} (u_Z - u) - M_{WY}$$

where

u_Z = x direction displacement at Z

v_Z = y direction displacement at Z

M_{WY} = Moment at Y axis due to intermediate load only

M_{WX} = Moment at X axis due to intermediate load only

Expressions for u_Z and v_Z may be written down as below after solution of the appropriate differential equation, viz.

$$u_Z = \Omega_Y \{\bar{A}_Y.Z + \bar{B}_Y + \bar{C}_Y.\sin \bar{m}_Y.Z + \bar{D}_Y.\cos \bar{m}_Y.Z$$

$$+ \frac{1}{\bar{m}_Y} \sin \bar{m}_Y.Z \int_0^Z (H_1 + Z)^{n+2} \cos \bar{m}_Y.Z.dZ$$

$$- \frac{1}{\bar{m}_Y} \cos \bar{m}_Y.Z \int_0^Z (H_1 + Z)^{n+2} \sin \bar{m}_Y.Z.dZ\}$$

and v_Z = As above with suffix 'X' throughout instead of 'Y'.

Definition of Symbols:

$$\Omega_Y = \frac{k_w \cos \gamma}{(n+1)(n+2)EI_Y} \; ; \qquad \Omega_X = \frac{k_w \sin \gamma}{(n+1)(n+2)EI_X}$$

$$\bar{B}_Y = B_Y + \frac{\bar{N}_Y (\sin \bar{m}_Y \ell - \bar{m}_Y \ell) + \bar{M}_Y . \bar{m}_Y (1 - \cos \bar{m}_Y \ell)}{\bar{m}_Y (2(1 - \cos \bar{m}_Y \ell) - \bar{m}_Y \ell \sin \bar{m}_Y \ell)}$$

$\bar{B}_X$ = As above with suffix 'X' throughout

$$\bar{C}_Y = C_Y + \frac{\bar{M}_Y . \bar{m}_Y \sin \bar{m}_Y \ell - \bar{N}_Y (1 - \cos \bar{m}_Y \ell)}{\bar{m}_Y (2(1 - \cos \bar{m}_Y \ell) - \bar{m}_Y \ell \sin \bar{m}_Y \ell)}$$

$\bar{C}_X$ = As above with suffix 'X' throughout

$$\bar{A}_Y = \phi_{Y1}/\Omega_Y - \bar{C}_Y . \bar{m}_Y \; ; \qquad \bar{A}_X = \phi_{X1}/\Omega_X - \bar{C}_X . \bar{m}_X$$

$$D_Y = u_1/\Omega_Y - \bar{B}_Y \; ; \qquad \bar{D}_X = v_1/\Omega_X - \bar{B}_X$$

$\bar{M}_Y$, $\bar{M}_X$, $\bar{N}_Y$, $\bar{N}_X$ in the above are defined as below:

$$\bar{M}_Y = \frac{1}{\Omega_Y} \{u_2 - u_1 \cos \bar{m}_Y \ell - \phi_{Y_1} \ell\}$$

$$\bar{M}_X = \frac{1}{\Omega_X} \{v_2 - v_1 \cos \bar{m}_X \ell - \phi_{X1} \ell\}$$

$$\bar{N}_Y = \frac{1}{\Omega_Y} \{\phi_{Y2} - \phi_{Y1} + u_1 \bar{m}_Y \sin \bar{m}_Y \ell\}$$

$$\bar{N}_X = \frac{1}{\Omega_X} \{\phi_{X2} - \phi_{X1} + v_1 \bar{m}_X \sin \bar{m}_X \ell\}$$

CIVIL ENGINEERING RESEARCH REPORTS

CE No.	Title	Author(s)	Date
1	Flood Frequency Analysis: Logistic Method for Incorporating Probable Maximum Flood	BRADY, D.K.	February, 1979
2	Adjustment of Phreatic Line in Seepage Analysis by Finite Element Method	ISAACS, L.T.	March, 1979
3	Creep Buckling of Reinforced Concrete Columns	BEHAN, J.E. & O'CONNOR, C.	April, 1979
4	Buckling Properties of Monosymmetric I-Beams	KITIPORNCHAI, S. & TRAHAIR, N.S.	May, 1979
5	Elasto-Plastic Analysis of Cable Net Structures	MEEK, J.L. & BROWN, P.L.D.	November, 1979
6	A Critical State Soil Model for Cyclic Loading	CARTER, J.P., BOOKER, J.R. & WROTH, C.P.	December, 1979
7	Resistance to Flow in Irregular Channels	KAZEMIPOUR, A.K. & APELT, C.J.	February, 1980
8	An Appraisal of the Ontario Equivalent Base Length	O'CONNOR, C.	February, 1980
9	Shape Effects on Resistance to Flow in Smooth Rectangular Channels	KAZEMIPOUR, A.K. & APELT, C.J.	April, 1980
10	The Analysis of Thermal Stress Involving Non-Linear Material Behaviour	BEER, G. & MEEK, J.L.	April, 1980
11	Buckling Approximations for Laterally Continuous Elastic I-Beams	DUX, P.F. & KITIPORNCHAI, S.	April, 1980
12	A Second Generation Frontal Solution Program	BEER, G.	May, 1980
13	Combined Stiffness for Beam and Column Braces	O'CONNOR, C.	May, 1980
14	Beaches:- Profiles, Processes and Permeability	GOURLAY, M.R.	June, 1980
15	Buckling of Plates and Shells Using Sub-Space Iteration	MEEK, J.L. & TRANBERG, W.F.C.	July, 1980
16	The Solution of Forced Vibration Problems by the Finite Integral Method	SWANNELL, P.	August, 1980
17	Numerical Solution of a Special Seepage Infiltration Problem	ISAACS, L.T.	September, 1980
18	Shape Effects on Resistance to Flow in Smooth Semi-circular Channels	KAZEMIPOUR, A.K. & APELT, C.J.	November, 1980
19	The Design of Single Angle Struts	WOOLCOCK, S.T. & KITIPORNCHAI, S.	December, 1980

CIVIL ENGINEERING RESEARCH REPORTS

CE No.	Title	Author(s)	Date
20	Consolidation of Axi-symmetric Bodies Subjected to Non Axi-symmetric Loading	CARTER, J.P. & BOOKER, J.R.	January, 1981
21	Truck Suspension Models	KUNJAMBOO, K.K. & O'CONNOR, C.	February, 1981
22	Elastic Consolidation Around a Deep Circular Tunnel	CARTER, J.P. & BOOKER, J.R.	March, 1981
23	An Experimental Study of Blockage Effects on Some Bluff Profiles	WEST, G.S.	April, 1981
24	Inelastic Beam Buckling Experiments	DUX, P.F. & KITIPORNCHAI, S.	May, 1981
25	Critical Assessment of the International Estimates for Relaxation Losses in Prestressing Strands	KORETSKY, A.V. & PRITCHARD, R.W.	June, 1981
26	Some Predications of the Non-homogenous Behaviour of Clay in the Triaxial Test	CARTER, J.P.	July, 1981
27	The Finite Integral Method in Dynamic Analysis : A Reappraisal	SWANNELL, P.	August, 1981
28	Effects of Laminar Boundary Layer on a Model Broad-Crested Weir	ISAACS, L.T.	September, 1981
29	Blockage and Aspect Ratio Effects on Flow Past a Circular Cylinder for $10^4 < R < 10^5$	WEST, G.S. & APELT, C.J.	October, 1981
30	Time Dependent Deformation in Prestressed Concrete Girder: Measurement and Prediction	SOKAL, Y.J. & TYRER, P.	November, 1981
31	Non-uniform Alongshore Currents and Sediment Transport - a One Dimensional Approach	GOURLAY, M.R.	January, 1982
32	A Theoretical Study of Pore Water Pressures Developed in Hydraulic Fill in Mine Stopes	ISAACS, L.T. & CARTER, J.P.	February, 1982
33	Residential Location Choice Modelling: Gaussian Distributed Stochastic Utility Functions	GRIGG, T.J.	July, 1982
34	The Dynamic Characteristics of Some Low Pressure Transducers	WEST, G.S.	August, 1982
35	Spatial Choice Modelling with Mutually Dependent Alternatives: Logit Distributed Stochastic Utility Functions	GRIGG, T.J.	September, 1982
36	Buckling Approximations for Inelastic Beams	DUX, P.F. & KITIPORNCHAI, S.	October, 1982

CIVIL ENGINEERING RESEARCH REPORTS

CE No.	Title	Author(s)	Date
37	Parameters of the Retail Trade Model: A Utility Based Interpretation	GRIGG, T.J.	October, 1982
38	Seepage Flow across a Discontinuity in Hydraulic Conductivity	ISAACS, L.T.	December, 1982
39	Probabilistic Versions of the Short-run Herbert-Stevens Model	GRIGG, T.J.	December, 1982
40	Quantification of Sewage Odours	KOE, L. & BRADY, D.K.	January, 1983
41	The Behaviour of Cylindrical Guyed Stacks Subjected to Pseudo-Static Wind Loads	SWANNELL, P.	March, 1983
42	Buckling and Bracing of Cantilevers	KITIPORNCHAI, S, DUX, P.F. & RICHTER, N.J.	April, 1983

CURRENT CIVIL ENGINEERING BULLETINS

4 *Brittle Fracture of Steel — Performance of ND1B and SAA A1 structural steels: C. O'Connor (1964)*

5 *Buckling in Steel Structures — 1. The use of a characteristic imperfect shape and its application to the buckling of an isolated column: C. O'Connor (1965)*

6 *Buckling in Steel Structures — 2. The use of a characteristic imperfect shape in the design of determinate plane trusses against buckling in their plane: C. O'Connor (1965)*

7 *Wave Generated Currents — Some observations made in fixed bed hydraulic models: M.R. Gourlay (1965)*

8 *Brittle Fracture of Steel — 2. Theoretical stress distributions in a partially yielded, non-uniform, polycrystalline material: C. O'Connor (1966)*

9 *Analysis by Computer — Programmes for frame and grid structures: J.L. Meek (1967)*

10 *Force Analysis of Fixed Support Rigid Frames: J.L. Meek and R. Owen (1968)*

11 *Analysis by Computer — Axisymetric solution of elasto-plastic problems by finite element methods: J.L. Meek and G. Carey (1969)*

12 *Ground Water Hydrology: J.R. Watkins (1969)*

13 *Land use prediction in transportation planning: S. Golding and K.B. Davidson (1969)*

14 *Finite Element Methods — Two dimensional seepage with a free surface: L.T. Isaacs (1971)*

15 *Transportation Gravity Models: A.T.C. Philbrick (1971)*

16 *Wave Climate at Moffat Beach: M.R. Gourlay (1973)*

17. *Quantitative Evaluation of Traffic Assignment Methods: C. Lucas and K.B. Davidson (1974)*

18 *Planning and Evaluation of a High Speed Brisbane-Gold Coast Rail Link: K.B. Davidson, et al. (1974)*

19 *Brisbane Airport Development Floodway Studies: C.J. Apelt (1977)*

20 *Numbers of Engineering Graduates in Queensland: C. O'Connor (1977)*